Laccase/TEMPO-mediated bacterial cellulose functionalization: production of paper-silver nanoparticles composite with antimicrobial activity

A. Gala Morena[a,c] M. Blanca Roncero[b], Susana V. Valenzuela[a,d], Cristina Valls[b], Teresa Vidal[b], F.I. Javier Pastor[a,d], Pilar Diaz[a,d] and Josefina Martínez*[a,d]

[a] Department of Genetics, Microbiology and Statistics, Faculty of Biology, Universitat de Barcelona, Av. Diagonal 643, 08028, Barcelona, Spain
[b] CELBIOTECH_Paper Engineering Research Group, EGE Department, Universitat Politècnica de Catalunya, Barcelona Tech, 08222, Terrassa, Spain
[c] Molecular and Industrial Biotechnology Group, Department of Chemical Engineering, Universitat Politècnica de Catalunya, Rambla Sant Nebridi 22, 08222 Terrassa, Spain
[d] Institute of Nanoscience and Nanotechnology (IN2UB), Universitat de Barcelona, Spain

*Corresponding author: Josefina Martínez. Department of Genetics, Microbiology and Statistics, Faculty of Biology, Universitat de Barcelona, Av. Diagonal 643, 08028 Barcelona, Spain. e-mail: jmartinez@ub.edu. Phone: +34 934034625.

A. Gala Morena angela.gala.morena@upc.edu (0000-0003-4470-8249)
M. Blanca Roncero blanca.roncero@upc.edu (0000-0002-2694-2368)
Susana V. Valenzuela susanavalenzuela@ub.edu (0000-0002-1684-9514)
Cristina Valls cristina.valls@upc.edu (0000-0003-2307-1779)
Teresa Vidal teresa.vidal@upc.edu (0000-0001-6269-4114)
F.I. Javier Pastor fpastor@ub.edu (0000-0003-0326-2527)
Pilar Diaz pdiaz@ub.edu (0000-0003-4008-0669)
Josefina Martínez jmartinez@ub.edu (0000-0002-2411-8188)

Abstract

Bacterial cellulose (BC) was functionalized applying the Laccase/TEMPO oxidative treatment, leading to a five-fold increase of the concentration of carboxyl groups. Paper produced with this cellulose showed improved mechanical properties while maintaining barrier function against water and greases as compared to paper produced with non-oxidized BC. Also, the negative charge provided by the carboxyl groups on functionalized BC was used to generate silver nanoparticles (AgNPs), obtaining a BC paper and Ag composite. The presence of AgNPs in the composites was validated by SEM, EDS and ICP analysis, showing spherical, uniformly sized particles stabilized in the BC nanofibers matrix. Additionally, antimicrobial property of composites containing AgNPs was tested. The results showed the strong antimicrobial activity of the composites against Gram-positive and Gram-negative bacteria and fungi. The generation of Ag nanoparticles in a matrix that combine the physical characteristics of the BC nanofibers with the stiffness and the mechanical properties of paper produced composites that may have applicability in technological and biomedical uses.

Keywords: Bacterial cellulose oxidation, laccase, bacterial cellulose paper, nanocomposite, silver nanoparticle, antimicrobial activity

Introduction

Bacterial cellulose (BC) is a biopolymer produced by some microorganisms, especially from the genera *Komagataeibacter*. In terms of chemical structure, BC is identical to the cellulose produced by vascular plants, composed by units of glucose linked by β(1→4)–glycosidic bonds. However, unlike vegetable cellulose, which is always bound to hemicellulose and lignin, BC is chemically pure (Chawla et al. 2009). The mechanical properties and microstructure of BC differ from those of vegetable cellulose. BC displays a higher degree of crystallinity, a higher

55 tensile strength, a higher water-holding capacity, and a finer three-dimensional nanofiber
56 network (Yano et al. 2005; Lee et al. 2014). The structural features and mechanical properties
57 are significant for practical application of BC. It can be used as a biomaterial for cosmetics
58 (Hasan et al. 2012; UllahSantos et al. 2016) and medical devices (Gao et al. 2011; Bielecki et al.
59 2012; Nimeskern et al. 2013; Ul-Islam et al. 2015; Stumpf et al. 2018;) as a reinforcement of
60 polymeric materials or paper (Miao et al. 2013; Fillat et al. 2018;), and as a material for food
61 packaging (Spence et al. 2010; Wu et al. 2018).

62 The chemical modification of the molecule is frequently a prerequisite to provide new
63 functions and applicability to cellulose (Rol et al. 2019). The functionalization of plant cellulose
64 by the oxidation of the C-6 carbon of glucose unites is known to improve some physical
65 characteristics of the paper such as the wet strength development (Kitaoka et al. 1999; Saito et
66 al. 2005, 2006). The most common procedure to selective oxidation of C-6 primary hydroxyl to
67 carboxyl or aldehyde groups in cellulose is through the radical 2,2,6,6–tetramethylpiperidine–
68 1–oxyl (TEMPO) combined with NaBr/NaOCl under alkaline conditions (Saito et al. 2004; Gert
69 et al. 2005). This is a well-established treatment widely used in vegetal cellulose (Isogai et al.
70 2011) and also has been recently attempted in bacterial cellulose (Lai et al. 2013; Feng et al.
71 2014; Pahlevan et al. 2018). The rate of these reactions is remarkably high, but the treatment
72 presents some disadvantages such as the undesirable de-polymerization of the cellulose, the
73 harsh conditions of the reaction, and the generation of chemical residues (Isogai et al. 2011).
74 The use of enzyme technology in industrial processes can reduce its negative environmental
75 and economic impact. The Laccase/TEMPO mediated oxidation operates in milder conditions
76 than the TEMPO/NaBr/NaClO treatment generating less environmental harmful residues, and
77 it has been successfully performed on vegetal cellulose (Aracri et al. 2011; Aracri and Vidal
78 2012; Aracri et al. 2012; Jiang et al. 2017; Quintana et al. 2017).

79 Once the cellulose is oxidized and new functional groups are created, compounds can be
80 added in order to provide new functionalities or to generate new composites (Johnson et al.
81 2011). Carboxyl groups have been used as host groups to introduce metal ions by an ion-
82 exchange reaction (Saito et al. 2005; Matsumoto et al. 2006;). Metal nanoparticles have been
83 proposed in different catalytic, photoelectric, magnetic, sensor, and biomedical applications
84 due to their electronic, optical, and chemical properties (Zhou et al. 2003; Sondi et al. 2004;
85 Jun et al. 2007; Wu et al. 2008). An essential issue with the synthesis and stabilization of metal
86 nanoparticles is their strong tendency to aggregate, losing their nanoscale characteristics. One
87 effective approach to prevent aggregation is the immobilization of the nanoparticles in a
88 polymeric insoluble matrix. The BC membranes have been used as nanoreactors for the
89 generation of silver nanoparticles (AgNPs). The hydroxyl groups and ether oxygen of the
90 cellulose molecule anchor the silver ions *via* ion-dipole interaction and, once reduced, form
91 stabilized nanoparticles in the fine nanofiber network (Maneerung et al. 2008; Pinto et al.
92 2009; Barud et al. 2011; Yang et al. 2012). The chemical oxidation with TEMPO of BC
93 membranes to generate carboxyl groups has been reported to increase the bounding strength
94 between the cellulose fibers and the silver ions, achieving a higher yield and a more uniform
95 distribution of the metal nanoparticles (Ifuku et al. 2009; Jin Feng et al. 2014). Recently, the
96 generation of aldehyde groups in BC by the hybrid system Laccase/ TEMPO oxidation of BC to
97 obtain aldehyde groups has been reported (Zhou et al. 2017) and its capability of further
98 oxidation to carboxyl groups would be expected. Moreover, in the AgNPs/BC composites
99 described so far, the metal nanoparticles are contained in membranes of BC. The implantation
100 of Ag nanoparticles in a matrix that combine the high surface-to-volume ratio of the BC
101 nanofibers with the stiffness and the mechanical properties of paper would generate a
102 composite with extended applicability.

103 The purpose of this study was to develop BC paper with good mechanical properties from
104 bacterial cellulose oxidized with the milder condition treatment Laccase/TEMPO. Furthermore,

we investigated the suitability of the bacterial cellulose functionalized with carboxyl groups to obtain silver nanoparticles on a solid stiff organic matrix and their antimicrobial activity.

Experimental

Materials

Microbial strains *Komagataeibacter xylinus* CECT 7351, *Staphylococcus aureus* CECT 234, *Pseudomonas aeruginosa* PAO1 CR321, *Klebsiella pneumoniae* CECT 143 and *Candida albicans* CECT 1001 were obtained from the Spanish Type Culture Collection (CECT). Peptone, Yeast extract, Luria Bertani broth (LB), Triptone Soy Agar (TSA) and Bacteriologic Agar were purchased from Laboratiorios Conda. Citric acid and disodium hydrogen phosphate (Na_2HPO_4) were purchased from Emsure. Glucose was purchased from PanReac. Silver nitrate, sodium hydroxide anhydrate pellet, sodium chloride and 2,2,6,6–tetramethyl–1–piperidinyloxy (TEMPO) and resazurin were purchased from Sigma Aldrich. Laccase from *Trametes villosa* with an activity of 746 U/mL was supplied by Novozymes.

Production of bacterial cellulose

To produce bacterial cellulose, *Komagataeibacter xylinus* was grown on the Hestrin and Schramm (HS) medium, containing 20 g/L glucose, 20 g/L peptone, 10 g/L yeast extract, 1.15 g/L citric acid, 6.8 g/L Na_2HPO_4, pH 6. Inoculum for culture was prepared by transferring *K. xylinus* cells grown on HS–Agar to HS liquid medium. After shaking vigorously, the resulting cell suspension was used to inoculate (1:40) 10 cm–Petri dishes containing 40 mL of HS medium. The cultures were statically incubated at 25–28°C for 7 days. After incubation, bacterial cellulose pellicles generated in the air/liquid interface of the culture media were harvested, rinsed with water, and purified by incubating them in 1 % NaOH at 70°C overnight. Finally, the BC pellicles were thoroughly washed in deionized water until the pH reached neutrality. To

obtain the bacterial cellulose suspension, pellicles were mechanically cut into small pieces and disrupted with a homogenizer (Homogenizing System UNIDRIVE X1000).

Laccase/TEMPO oxidation

Laccase/TEMPO oxidation was adapted from earlier studies carried out in vegetable cellulosic fibers (Aracri et al. 2012; Aracri et al. 2011; Quintana et al. 2017). The treatment was performed at room temperature in a 50 mM acetate buffer at pH 5, in the dark. TEMPO (8% w/w) and Laccase (60 U/dry gram of BC) were added to the 5% consistency BC suspension. The blend was mechanically mixed until the components were totally homogenized and then kept at room temperature for 24 h. After the treatment, the functionalized BC suspension was filtered and washed with deionized water. These oxidized BC samples were named as BC–ox.

Quantification of carboxyl and aldehyde groups

Carboxyl and aldehyde groups were measured in the initial and oxidized BC samples. Quantification of carboxyl groups (COOH) was performed by the methylene blue dye test. Briefly, this method is based on the following ion exchange reaction (Equation 1):

$$\mathrm{R-COOH + Mb^{+} \leftrightarrow R-COOMb + H^{+}} \quad (1)$$

where Mb^{+} represents the methylene blue ions in dye solution (Davidson 1948).

For the analysis, 0.05 dry grams of sample were suspended in 50 mL of a 0.2 mM solution of methylene blue. After 24 h of stirring in the dark, the sample was passed through a glass filter. The filtrate was centrifuged at 3,000 rpm for 20 minutes. The supernatant was diluted 1:25 and analyzed using UV spectroscopy (Type Evolution 600 BB, Thermo Scientific) at 664 nm. The concentration of carboxyl groups (µmol per dry gram of BC) was estimated through the Equation 2 and using a calibration curve:

$$\text{Concentration of COOH groups } (\mu\text{mol/g}) = \frac{(c-c')\cdot 0.05\cdot 1000}{m+p-m'} \quad (2)$$

where *c* is the initial concentration of methylene blue, *c'* is the concentration of methylene blue after the reaction, *p* is the dry weight of the sample, *m* is the weight of the glass filter, and *m'* is the weight of the glass filter after the filtration.

Quantification of aldehyde groups (CHO) was performed by the methylene blue dye test, using 0.25 dry grams of sample. Prior to the measurement, the samples were introduced into 25 mL of sodium chlorite. The mixture was incubated for 24 h, stirring in the dark. The concentration of aldehyde groups can be determined by Equation 3:

$$\text{Concentration of CHO groups } (\mu\text{mol/g}) = \text{COOH}_{\text{AO}} - \text{COOH}_{\text{BO}} \quad (3)$$

where $COOH_{AO}$ is the content of carboxyl groups(μmol/g) after the oxidation with sodium chlorite and $COOH_{BO}$ is the content of carboxyl groups (μmol/g) before the oxidation with sodium chlorite.

BC paper sheet formation and physical and mechanical properties characterization

Bacterial cellulose sheets were produced using a Rapid–Köthen laboratory former (Frank–PTI) following the ISO–5269:2004 standard method. Sheets were conditioned at 23°C and 50% of relative humidity for at least 24 h before physical and mechanical testing, as indicated in ISO 187. Physical and mechanical properties were measured according with standards indicated in parenthesis as follow: density (ISO 534), brightness (UNE 57060), opacity (UNE 57063), water drop test (tappi T835 om-08), grease resistance (UNE 57071), and wet tensile index (ISO 1924-2).

Formation of composites of paper containing silver nanoparticles

Oxidized BC suspension was soaked in a 10 mM or 0.1 mM $AgNO_3$ solution in a 1:1 ratio (BC wet weight : $AgNO_3$ solution volume). The mixture was mechanically homogenized and incubated in the dark, at room temperature for 24 hours. After the incubation, the treated BC was rinsed with water and filtered through a glass filter to remove the excess of $AgNO_3$. Following the formation of BC paper sheets, a thermal treatment at 121°C for 20 minutes was applied to induce the reduction of Ag ions and promote the formation of AgNPs (Fig. 1). For simplicity, the composites of paper generated with 10 mM and 0.1 mM $AgNO_3$ will be referred as BC-ox-10Ag and BC-ox-0.1Ag throughout respectively.

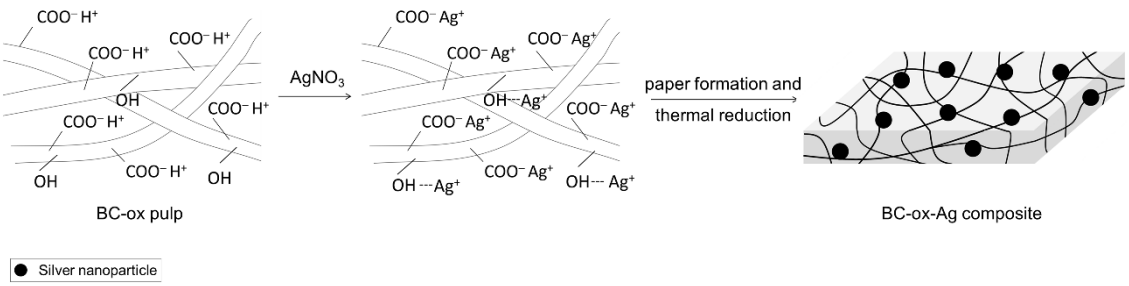

Fig. 1 Schematic model of silver nanoparticles generation in BC composites after oxidation treatment

Scanning Electron Microscope (SEM) and Energy Dispersive X–ray Spectroscopy (EDS) analysis

The presence of nanoparticles in BC-ox-Ag composites was verified by SEM (JSM 7100 F) using a LED filter and a backscattered electron detector (BED). EDS analysis was carried out to verify the chemical composition of the nanoparticles. The diameter of the nanoparticles was measured using the ImageJ software.

Ag migration from the composites

To measure the diffusion of silver from the BC matrix, the composites were cut into square pieces of 1 cm^2, immersed into 1 mL of deionized water, and incubated at room temperature while shaken at 1000 rpm during 24 h. Then, the composites were removed and the silver content in the water was analyzed by inductively coupled plasma mass spectrometry (ICP-MS). The Ag content of the samples was analyzed both before and after the addition of HNO_3 at a final concentration of 1%. The acid dissolves the AgNPs to Ag ions prior to ICP-MS analysis.

Antimicrobial activity of the composites containing silver nanoparticles (BC-ox-Ag)

The antimicrobial properties of BC-ox-Ag composites were tested against the Gram-positive bacteria *Staphylococcus aureus*, the Gram-negative bacteria *Pseudomonas aeruginosa* and *Klebsiella pneumoniae,* and the yeast *Candida albicans*. To obtain the inoculum for the antimicrobial tests, the strains were grown overnight in LB broth at 37°C in shaking conditions. The overnight cultures were centrifuged for 4 minutes at 14000 *xg* and the pellet suspended in 0.3 mM KH_2PO_4 (hereinafter work solution) to remove the culture medium. Both, BC-ox-Ag composites and BC paper were cut in squares of 1 cm^2 and sterilized prior to the assay. Two antimicrobial tests were performed, the *Drop over paper test* and the *Dynamic contact condition test*.

Drop over paper test

3 µl of the corresponding microbial suspension (about 10^5 microorganisms per mL) were inoculated over the 1 cm^2 BC-ox-Ag composites placed on the surface of TSA medium plates. The growth over a sample of BC paper was used as positive control. After overnight incubation at 37°C, the microorganisms were detached from the composites and BC paper by intense shaking on the work solution, and the metabolic activity of the resuspension was measured by

the resazurin assay. For the assay, 50 µL of resazurin (7–Hydroxy–3H–phenoxazin–3–one–10–oxide) were added to 100 µL of each microbial resuspension in a 96–well plate. The plate was incubated at 37°C in dark conditions until the solution turned pink (approximately 10 minutes). Fluorescence was measured with Varian Cary Eclipse Fluorescence Spectrophotometer. The difference between the metabolic activity of the microorganisms grown on BC-ox-Ag composites and on BC paper was used to calculate the percentage of growth inhibition.

Dynamic contact conditions test

This procedure was adapted from ASTM E2149–01 (*Standard test Method for determining the antimicrobial activity agents under dynamic contact conditions*). Nine 1 cm^2 pieces of the composites were immersed in 5 mL of a suspension of a known concentration of microorganisms and incubated at room temperature while stirred. In each case, a control was run with the BC paper under the same conditions. The viable cells on the suspension were determined at different times (0, 1, 4 and 24 h). The percentage of reduction was calculated by Equation 4:

$$\%\ \text{cell viability reducion} = \frac{\text{viable CFU at } t_0 - \text{viable CFU at } t_x}{\text{viable CFU at } t_0} \times 100 \qquad (4)$$

where t_0 is the time 0 h and t_x is the time at which the percentage of reduction is calculated.

Results and discussion

Laccase/TEMPO oxidation

BC suspension was treated with Laccase/TEMPO to oxidize the hydroxyl groups of cellulose molecules and to introduce functional carboxyl groups. The enzyme Laccase catalyzes the oxidation of the TEMPO molecule. The oxidized TEMPO radical, in turn, oxidizes the primary alcohols in cellulose to carboxyl (COOH) and aldehyde (CHO) functional groups (Aracri et al.

245 2011). Fig. 2 shows the content of carboxyl and aldehyde groups of BC molecule before (BC)

246 and after Laccase /TEMPO oxidation (BC-ox) with 8% TEMPO and 60 U/g Laccase.

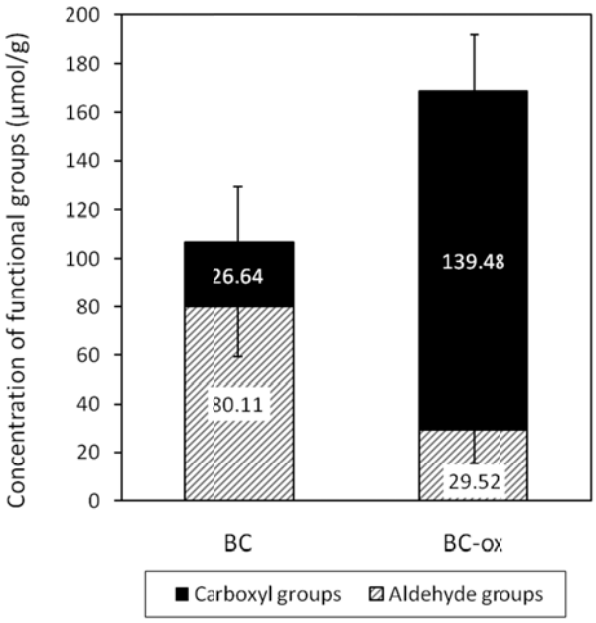

246

248 **Fig. 2** Carboxyl and aldehyde groups (µmol/g cellulose) of bacterial cellulose (BC) and oxidized
249 bacterial cellulose with the Laccase/TEMPO treatment (BC-ox)

249

259 Results showed that the amount of carboxyl groups increased from 26.6 µmol/g to 139.5

260 µmol/g after the oxidation, which is five times more than the initial value. The presence of

261 carboxyl and aldehyde groups in the BC molecule before the Laccase/TEMPO treatment could

262 be due to the oxidation of cellulose by unspecific physical factors, such as visible light (Tolvaj et

263 al. 1995), or during the isolation and purification procedures (Jaušovec et al. 2015). After the

264 treatment, the concentration of aldehyde groups decreased because part of these aldehyde

265 groups was oxidized to carboxyl groups by action of Laccase/TEMPO. Thus, the results

266 suggested that some of the carboxyl groups detected were induced from aldehyde groups

267 initially present in BC, while other were generated *de novo* from new aldehyde groups which,

268 in turn, were induced from primary alcohol groups present in BC.

Previous studies have shown that the TEMPO/NaBr/NaClO oxidation treatment of cellulose was efficient generating carboxyl groups. Milanovic et al. reported an eight-fold increase of the COOH amount in cotton fibers after TEMPO/NaBr/NaClO (Milanović et al. 2016), while Gehmayr et al. achieved an eleven-fold increase in ECF eucalyptus kraft pulp (Gehmayr et al. 2012). The TEMPO/NaBr/NaClO procedure has been also successfully attempted in nanofibrillated cellulose from different plant cellulosic fibers (Chen et al. 2017). The studies reporting bacterial cellulose oxidized with TEMPO/NaBr/NaClO treatment found an efficiency similar to that previously referred to cellulose from plant (Ifuku et al. 2009; Wu et al. 2018). The Laccase/TEMPO mediated oxidation operates in milder conditions than the TEMPO/NaBr/NaClO treatment generating less environmental harmful residues and it has been successfully applied in plant cellulose, although with less efficiency. Quintana et al. reported a 6-fold increase of COOH groups in a refined dissolving pulp from plant cellulose after Laccase/TEMPO oxidation (Quintana et al. 2017). Likewise, Patel et al. oxidized cotton linters by Laccase/TEMPO and the carboxyl group content was 9 times higher than in the control sample (Patel et al. 2011). However, other authors reported an increase of the COOH content of only up to 2 or 3 times (Aracri et al. 2012; Aracri and Vidal 2012; Jaušovec et al. 2015). While the Laccase/TEMPO procedure has been previously applied to generate aldehyde groups in BC membranes (Zhou et al. 2017), this work assessed the oxidation to carboxyl groups. The results were comparable to those obtained in plant cellulose after Laccase/TEMPO mediated oxidation.

Characterization of paper sheets produced with oxidized BC

After the oxidation of BC, paper sheets were produced and compared with paper made from non-oxidized BC in terms of physical and mechanical properties to verify if the Laccase/TEMPO oxidation treatment affected those properties. Results are shown in Table 1.

284 Table 1. Physical and mechanical properties of oxidized BC (BC–ox) paper sheets and BC papers
285 sheets

Property	BC paper	BC–ox paper
Density (g/cm^3)	0.78	0.51
Brightness (%)	52.0 ± 1.6	54.4 ± 1.9
Opacity (%)	66.3 ± 1.8	65.6 ± 1.4
Water dropt test (WDT) (s)	2355 ± 102.5	2397 ± 89.6
Grease resistance (s)	>1800	>1800
Wet tensile index (kN·m/kg)	11.1 ± 4.3	15.1 ± 0.3
Wet tensile strength development (W/D) (%)	13.8	22.3

286

287 The oxidative treatment of BC did not affect brightness and opacity of the paper. Moreover,
288 values of WDT and grease resistance were similar in both BC and BC-ox sheets, indicating that
289 water and grease barrier properties were not modified by the Laccase/TEMPO treatment.
290 However, the strength properties varied in the two types of paper. The wet tensile strength
291 development is the increase of tensile resistance in wet paper in relation to dry paper, and it is
292 also known as ratio of wet versus dry tensile index (W/D). The wet strength is one of the most
293 important properties of papers that must be in contact with liquids, such as tissue paper,
294 paper towels, filter paper, packaging papers, etc. Paper made from BC-ox showed a 22.3% wet-
295 to-dry (W/D) strength ratio, whereas for paper made from BC, this value was 13.8%. Thus, the
296 Laccase/TEMPO treatment allowed the improvement of the wet strength development by
297 62%. The reported W/D value of BC-ox paper is a significant improvement, paper with values
298 over 15% are considered to have excellent wet tensile strength properties (Scott 1996). The
299 increase of wet strength obtained in BC-ox paper could be attributed to the formation of
300 hemiacetal bonds in cellulose, as suggested by Aracri et al. (2011).

301

Production and characterization of BC-ox-Ag composites

The suitability of the functionalized BC on the generation of paper sheets containing silver nanoparticles (BC-ox-Ag composites) was tested. Suspensions of BC-ox were mixed with 10 mM or 0.1 mM $AgNO_3$ solutions as a source of Ag ions. In the proper conditions, it would be expected that the negatively-charged BC molecules functionalized with carboxyl groups attract the Ag^+ cations *via* electrostatic interactions. In addition, electron-rich oxygen atoms resulting from hydroxyl and ester of the BC molecule could also contribute to keep stable the Ag ions in the BC nanofibers matrix (i.e., by ion-dipole interaction) (Barud et al. 2011). Then, with the obtained BC-ox-Ag mix, paper sheets were produced, and heat (121°C, 20 min) was used to trigger the reduction of Ag ions and consequently the formation of nanoparticles (Maria et al. 2010). It has been described that the complex formed between Ag and carboxyl groups could promote particle nucleation, anchoring the growing nanoparticle (de Santa Maria et al. 2009). The tri-dimensional structure of BC nanofibrils with very high specific surface area would help to stabilize the particles preventing agglomeration.

BC-ox-Ag composites were analyzed by scanning electron microscopy (SEM) and energy dispersive X-ray spectroscopy (EDS). Fig. 3 shows SEM images of the surface of BC paper and BC-ox-Ag composites produced with 10 mM $AgNO_3$ (BC-ox-10Ag) and 0.1 mM $AgNO_3$ (BC-ox-0.1Ag). Fig. 3a is an image of the surface of the paper produced with BC showing a typical network structure of ribbon-shaped cellulose fibrils of about 50-70 nm wide and several micrometers long. After treatment with 10 mM $AgNO_3$ and 0.1 mM $AgNO_3$, we observed the matrix of nanofibers with randomly distributed spherical nanoparticles attached to their surface (Fig. 3c and 3e, respectively). The same SEM fields observed with the BED–C filter showed the nanoparticles brightly highlighted (Fig. 3d and 3f), suggesting that they may be made of a high atomic weight element. As shown in Fig. 3c to 3f, both BC-ox-10Ag and BC-ox-

0.1Ag composites presented nanoparticles on the BC fiber surface, unlike on the BC paper (Fig. 3a and 3b).

The composition of the generated nanoparticles was further investigated by energy dispersive X–ray spectroscopy (EDS) analysis (Fig. 4). EDS of BC-ox-10Ag and BC-ox-0.1Ag composites indicated a strong signal corresponding to silver (white arrows in Fig. 4). Peaks of hydrogen, oxygen, and carbon in the spectrum correspond to components of the molecule of cellulose. The results confirmed that the spherical nanoparticles observed in SEM images of the BC composites were made of silver.

The average size of the nanoparticles was measured, resulting in diameters of 41.4 ± 2.4 nm and 51.4 ± 2.4 nm for BC-ox-10Ag and BC-ox-0.1Ag composites, respectively. The size of the nanoparticles was uniform in both cases. BC-ox-0.1Ag composites presented larger but less abundant nanoparticles than BC-ox-10Ag composites, as observed in microscope images (Fig. 3). These results could be explained by different dynamics in the silver nanoparticle formation depending on the ratio between silver ion concentration and the carboxyl groups available (Uddin et al. 2014). During the reduction process, the lowest concentration of Ag^+ (0.1 mM $AgNO_3$) could allow the nucleation of a limited number of stable clusters of metallic silver to form the nanoparticles. The remaining dissolved silver of the surroundings, that would not reach the nucleation threshold to cluster, would be absorbed into the growing nanoparticles (Perala et al. 2013) leading to larger sizes. In contrast, in 10 mM $AgNO_3$ solutions there would be enough concentration of silver ions to form of a larger number of stable clusters, but of smaller size.

The impregnation of BC membranes with Ag nanoparticles has been previously described to provide antimicrobial activity for wound healing applications (Inoue et al. 2010; UllahWahid et al. 2016; Chun-Nan Wu et al. 2018). In these studies, BC membranes were immersed in $AgNO_3$ solutions followed by the reduction of the Ag ion and the formation of the metal particles.

Often, additives such as protective colloids were used to control the formation and size distribution of the particles (Maneerung et al. 2008; Jalili Tabaii et al. 2018). BC membrane oxidized by the TEMPO chemical system has been used as a template to form AgNPs by thermal (Ifuku et al. 2009) or chemical (Jin Feng et al. 2014) reduction.

In agreement with the results obtained, the procedure employed here was efficient in forming spherical, uniformly sized AgNPs, without the inclusion of chemical reducing agents and stabilizers. This improves both the environmental aspect of the process, avoiding the secondary pollutants, and the reduction of the presence of residues in the nanocomposite that could interfere in its applicability, especially related to fields such as biomedicine and catalysis. Moreover, in this work AgNPs were generated in a dry, stiff, enduring paper with important properties for applications such as biocatalysis, biosensors, or packaging.

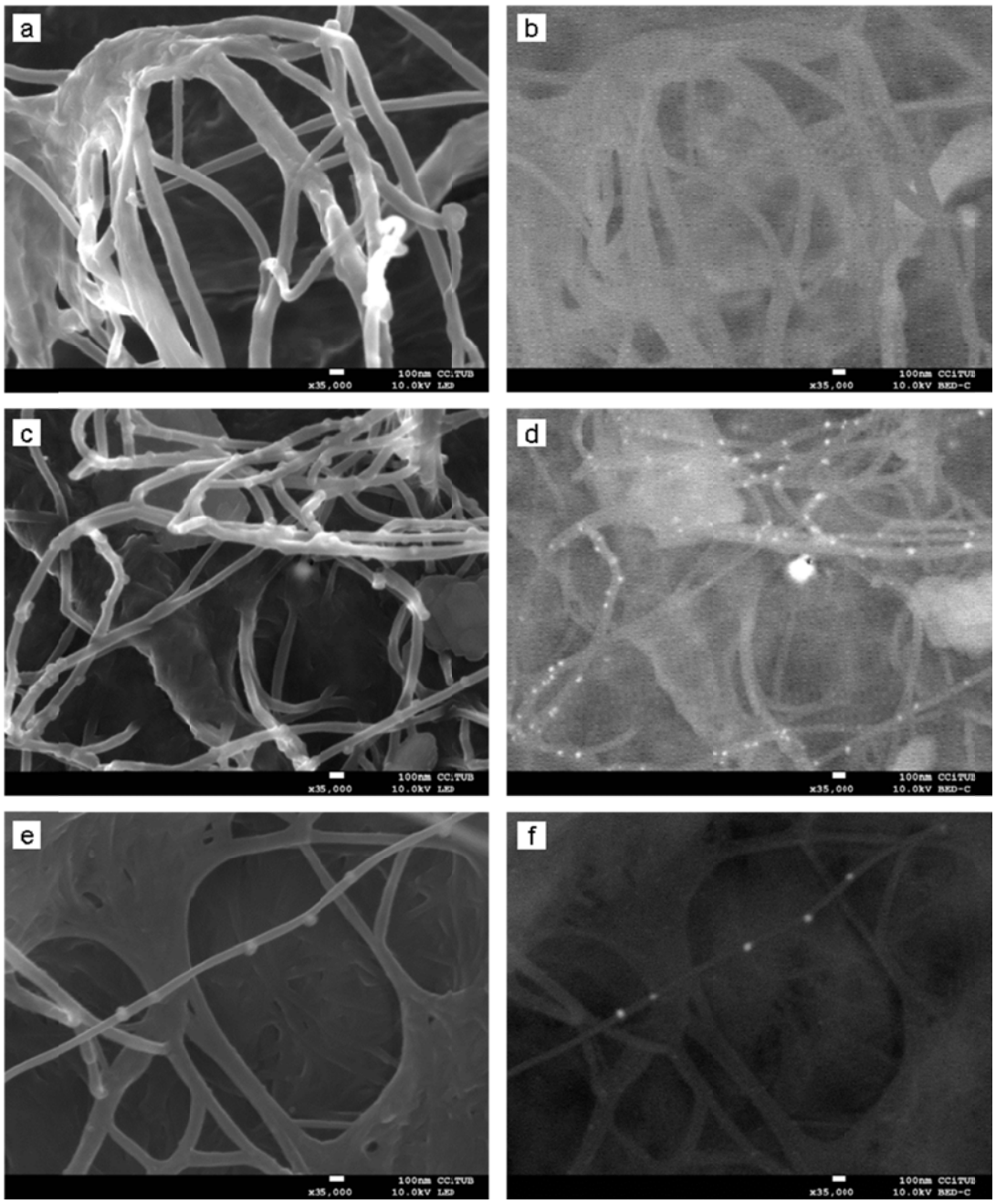

Fig. 3 SEM images of BC composites. (a) BC paper visualized with LED filter. (b) BC paper visualized with BED–C filter. (c) BC-ox-10Ag composites visualized with LED filter. (d) BC-ox-10Ag composites visualized with BED–C filter (e) BC-ox-0.1Ag composites visualized with LED filter. (f) BC-ox-0.1Ag composites visualized with BED–C filter

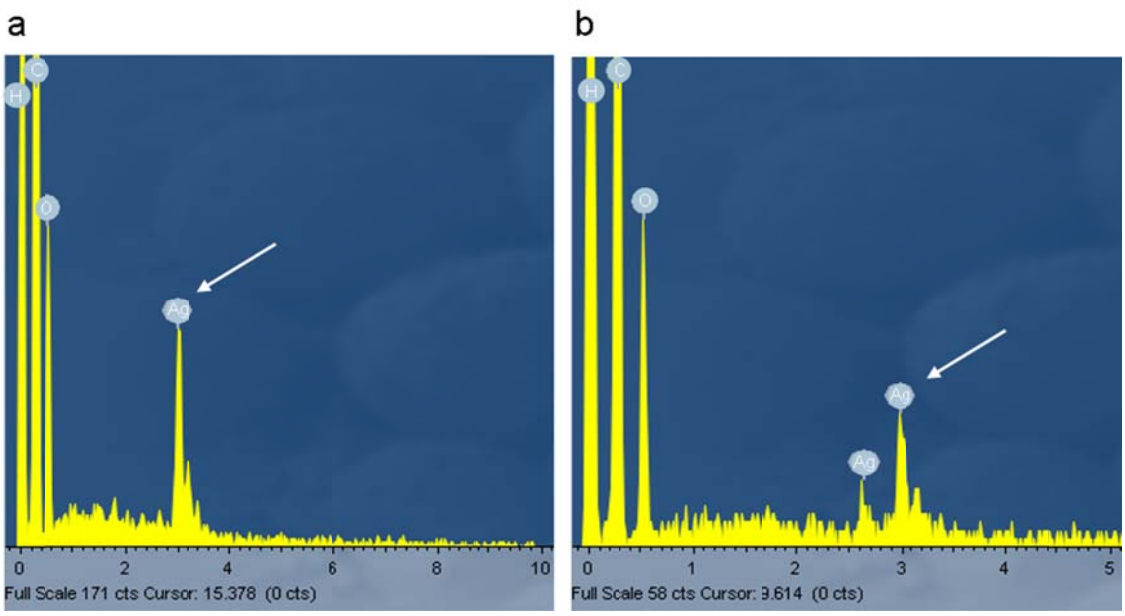

Fig. 4 Energy dispersive X–ray spectrometer (EDS) spectrum of silver nanoparticles in BC-ox-10Ag composite (a) and in BC-ox-0.1Ag composite (b). White arrows indicate the Ag peak in the spectrum

Silver release from BC-ox-Ag composites

The silver diffusion from the BC-matrix was analyzed to acquire further information regarding the properties of the composites. Composites which were not heat-treated to prevent the induction of AgNPs formation (BC-ox-10Ag-NR and BC-ox-0.1Ag-NR, in Table 2) were produced and compared with composites containing Ag nanoparticles (BC-ox-10Ag and BC-ox-0.1Ag, in Table 2). The composites were immersed and shaken in water for 24 h. Then, the silver content in the water was analyzed by inductively coupled plasma (ICP) (Table 2). Samples were analyzed both with and without the addition of HNO_3. Without the addition of HNO_3, the Ag released in form of ions was determined. The addition of HNO_3 allowed the digestion of the AgNPs to Ag ions prior to the ICP-MS analysis, thus retrieving the value of the total content of silver released by the matrix of the composites. The comparison of the values obtained for the same sample with and without the treatment with HNO_3 would allow the estimation of Ag released that was in form of nanoparticles.

386 Table 2. Silver migration from composites (ng Ag/mg composite)

Composite	Silver released in form of Ag ions	Total content of silver released
BC-ox-10Ag	4.65 ± 0.2	5.34 ± 0.3
BC-ox-10Ag-NR	16.42 ± 2.2	19.44 ± 3.7
BC-ox-0.1Ag	<0.1 (*)	0.23 ± 0.1
BC-ox-0.1Ag-NR	1.24 ± 0.2	1.92 ± 0.2

387 NR: not reduced. (*): Value below the detection limit of the method

388

389 Differences of the values comparing the silver released as ion with the total Ag release,
390 showing Table 2, were found not significant (t-Student, statistical confidence level 95 %). Thus,
391 for the composites containing AgNPs, the results indicated that most of the Ag present in the
392 analyzed samples was in the form of Ag ion, suggesting that silver was leached to the medium
393 in form of Ag ions diffused from the NPs inside the BC matrix, rather than in form of NPs.
394 Probably, the fine network of nanofibers of the BC matrix on the composite helps to stabilize
395 and to retain the NPs. Release of Ag from composites that were not submitted to heat
396 treatment, and therefore no NPs were generated (BC-ox-Ag NR), was greater than from its
397 counterpart composites (BC-ox-Ag) (Table 2), indicating that the chemical form in which the
398 silver was embedded in the BC matrix affected its diffusion into the surrounding aqueous
399 medium.

400 The fraction of silver released varied regarding the chemical form of Ag embedded in the BC
401 matrix (Fig. 5). For BC-ox-10Ag composites, 29 % of its silver content was diffused from the
402 matrix after 24 h immersed in the aqueous medium. However, the release of Ag increased to
403 94% for composites where the heat reduction treatment was not applied, indicating that the
404 reduction was necessary for the stabilization of Ag in the matrix, probably through the
405 generation of NPs.

406 Finally, we explored the importance of the BC oxidation on the silver release from the
407 composites prepared with non-oxidized BC pulp. As shown in Fig. 5, the diffusion of Ag from

non-oxidized composites (BC-10Ag) was significantly higher than that found in oxidized composites (BC-ox-10Ag). The difference could be attributed to the carboxyl groups induced by the laccase/TEMPO oxidation, which provided negative charges attracting Ag ions and promoting nucleation for NPs formation.

These results suggested that both steps, oxidation and heat treatment, were necessary to obtain BC composites containing silver nanoparticles stabilized in the matrix. The same conclusion was drawn from the results obtained using BC-ox-0.1Ag composite (data not shown). The stability of the nanoparticle inside the matrix as well as the diffusion of silver ions could have important implications for biomedical or food packaging applications (Marini et al. 2007; Kong et al. 2008; Maneerung et al. 2008).

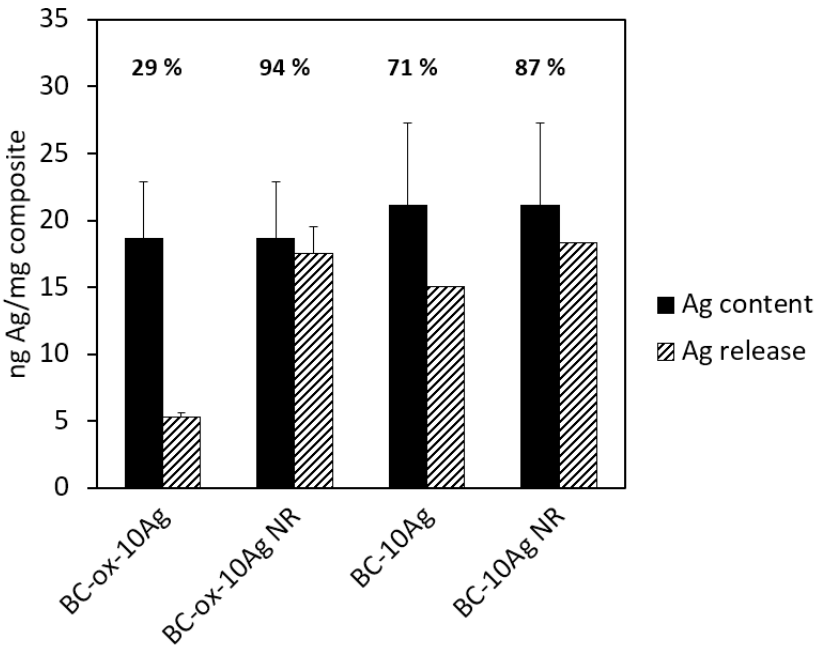

Fig. 5 Silver content and silver migration from the composites (ng Ag/mg composite). BC-ox-10Ag: composite produced with oxidized bacterial cellulose and 10 mM of silver nitrate; BC-10Ag: composite produced with non-oxidized bacterial cellulose and 10 mM of silver nitrate. NR: no thermal reduction applied. Percentages represent the fraction of silver released from each type of composite

Antimicrobial properties of BC-ox-Ag nanocomposites

The antimicrobial property of composites containing silver nanoparticles (BC-ox-Ag) was tested against Gram-positive bacteria (*S. aureus*), Gram-negative bacteria (*P. aeruginosa*, *K. pneumoniae*), and yeast (*C. albicans*).

The capability of the BC-ox-Ag composites to inhibit the microbial growth on their surface was assayed by the *drop over paper test*. Microbial metabolic activity was not detected after incubation in contact with BC-ox-10Ag and BC-ox-0.1Ag composites for any of the microorganisms tested, while all four strains were able to grow in contact with the BC paper sheet (results not shown).

To evaluate the bactericidal and fungicidal ability of the BC-ox-Ag composites under dynamic liquid condition, suspensions of microorganisms were incubated in contact with the composites. Viable cell counts were determined at different times, and the percentage of cell viability reduction was calculated (Table 3). Suspensions of the microorganisms in contact with samples of BC paper sheets did not experiment a decrease of viability over 24 h incubation time (results not shown). The reduction of viability after one hour of incubation with BC-ox-10Ag composites was over 90% for *S. aureus*, *P. aeruginosa* and *K. pneumoniae*, and complete loss of bacterial viability was obtained after 4 h (Table 3). For *C. albicans*, total elimination of 10^6 CFU/mL was not achieved after 24 h in contact with BC-ox-10Ag composite. These results demonstrated that BC-ox-10Ag composite presented strong biocidal activity against the tested strains, being more effective for bacteria than for yeast.

BC-ox-0.1Ag composites presented antibacterial properties as well, although unevenly for different types of microorganisms. Hence, contact with BC-ox-0.1Ag composites eliminated Gram-negative bacteria *P. aeruginosa* and *K. pneumoniae,* and reduced the viability of the Gram-positive *S. aureus* to 95 % after 24 h (Table 3). However, the viability of about 10^5 CFU/mL of the fungi *C. albicans* was not affected after 24 h. The differences observed between

450 the three types of microorganisms may be related to the structure of their cellular envelopes.
451 Thus, to some extent, thicker cell walls, such as those of *S. aureus* and *C. albicans*, would
452 protect the cell from the contact of silver ions with the cell membrane and their penetration
453 into the cytoplasm (Feng et al. 2000). Evidently, BC-ox-10Ag composites presented a further
454 pronounced antimicrobial property as they contain a larger amount of silver. BC membranes
455 containing silver nanoparticles have previously been reported to present antimicrobial activity
456 against *E. coli*, *S. aureus*, *K. pneumoniae* and *C. albicans* (Maneerung et al. 2008; Pinto et al.
457 2009; Shao et al. 2015; Jalili Tabaii et al. 2018). Silver has been used for centuries for the
458 treatment of burns and wounds. It has been reported that silver ions bind to the thiol groups
459 of proteins and the respiratory enzymes of the bacterial cell membrane (Liau et al. 1997; Feng
460 et al. 2000). However, the mechanism for its antimicrobial action is not completely
461 understood. Both silver ion and silver nanoparticles are toxic for microorganisms (Abdel-
462 Mohsen et al. 2014), although some authors maintain that the antimicrobial effect of the
463 nanoparticles derives from the release of silver ions (Lansdown 2006).

464 Table 3.Viable cell counts (CFU/mL) and cell viability reduction (%) of microorganisms in
465 dynamic contact with BC-ox-10Ag and BC-ox-0.1Ag composites.

		BC-ox-10Ag		BC-ox-0.1Ag	
		CFU/mL	% reduction	CFU/mL	% reduction
S. aureus	t_0	$2.5 \cdot 10^7$	0	$1.3 \cdot 10^6$	0,0
	t_1	$1.2 \cdot 10^6$	95.2	$5.4 \cdot 10^5$	57.9
	t_4	0	100	$1.8 \cdot 10^5$	84.5
	t_{24}	0	100	$5.7 \cdot 10^4$	95.6
P. aeruginosa	t_0	$1.4 \cdot 10^6$	0	$3.5 \cdot 10^5$	0
	t_1	$1.3 \cdot 10^5$	90.7	$2.7 \cdot 10^5$	5.3
	t_4	0	100	$1.92 \cdot 10^5$	45.1
	t_{24}	0	100	0	100
K. pneumoniae	t_0	$6.6 \cdot 10^5$	0	$3.5 \cdot 10^6$	0
	t_1	$2 \cdot 10^3$	99.7	$2.7 \cdot 10^6$	22.8
	t_4	0	100	$2.2 \cdot 10^6$	34.9
	t_{24}	0	100	0	100
C. albicans	t_0	$1.4 \cdot 10^6$	0	$5.9 \cdot 10^4$	0
	t_1	$7.6 \cdot 10^5$	47.2	$8.4 \cdot 10^4$	0
	t_4	$8 \cdot 10^5$	44.4	$1 \cdot 10^5$	0
	t_{24}	$4.6 \cdot 10^5$	69.8	$1 \cdot 10^5$	0

466

BC-ox-Ag composites produced in this work presented strong antimicrobial activity due to their silver nanoparticle content. The toxic action of the nanoparticles can be exerted both by direct contact of the microorganisms with the surface of the composite, and by the release of Ag ions in aqueous conditions. The composites suitability to inhibit the microbial growth in their surfaces as well as to eliminate bacteria and fungi in aqueous surroundings is a fundamental aspect to consider for future applications.

Conclusions

In this work the production of BC and Ag nanoparticles composites with paper mechanical features and excellent barrier properties was achieved. Carboxyl groups induced by the Laccase/TEMPO oxidation of BC nanofibers enabled the interaction with Ag ions and the generation of silver nanoparticles after thermal induction. BC matrix allowed the stabilization of evenly sized and shaped nanoparticles. Composites had antimicrobial activity, showing great capability to both inhibit growth and kill Gram-positive bacteria, Gram-negative bacteria, and fungi. It is foreseeable that composites with nanoparticles of other metals can be obtained by following the same method described here. BC paper composites containing metal nanoparticles could be employed in catalytic, magnetic, conductive, and biomedical applications.

Acknowledgements

This work was financed by the Spanish Ministry of Economy, Industry and Competitiveness, grant ref. MICROBIOCEL: CTQ2017-84966-C2-1-R and CTQ2017-84966-C2-2-R projects, FILMBIOCEL CTQ2016-77936-R (funding also from the “Fondo Europeo de Desarrollo Regional FEDER”), by the Pla de Recerca de Catalunya, grant 2017SGR-30, and by the Generalitat de

Catalunya, “Xarxa de Referència en Biotecnologia” (XRB). Special thanks are also due to the Serra Húnter Fellow to C. Valls.

Conflict of interest

The authors declare that they have no conflict of interest.

References

Abdel-Mohsen AM, Abdel-Rahman RM, Fouda MMG, Vojtova L, Uhrova L, Hassan AF, Al-Deyab SS, El-Shamy IE, Jancar J (2014) Preparation, characterization and cytotoxicity of schizophyllan/silver nanoparticle composite. Carbohydrate Polymers, 102(1), 238–245. https://doi.org/10.1016/j.carbpol.2013.11.040

Aracri E, Valls C, Vidal T (2012) Paper strength improvement by oxidative modification of sisal cellulose fibers with laccase–TEMPO system: Influence of the process variables. Carbohydrate Polymers, 88(3), 830–837. https://doi.org/10.1016/j.carbpol.2012.01.011

Aracri E, Vidal T (2012) Enhancing the effectiveness of a laccase–TEMPO treatment has a biorefining effect on sisal cellulose fibres. Cellulose, 19(3), 867–877. https://doi.org/10.1007/s10570-012-9686-4

Aracri E, Vidal T, Ragauskas AJ (2011) Wet strength development in sisal cellulose fibers by effect of a laccase–TEMPO treatment. Carbohydrate Polymers, 84(4), 1384–1390. https://doi.org/10.1016/j.carbpol.2011.01.046

Barud HS, Regiani T, Marques RFC, Lustri WR, Messaddeq Y, Ribeiro SJL (2011) Antimicrobial bacterial cellulose-silver nanoparticles composite membranes. Journal of Nanomaterials, 2011, 1–8. https://doi.org/10.1155/2011/721631

Bielecki S, Kalinowska H, Krystynowicz A, Kubiak K, Kołodziejczyk M, de Groeve M (2012) Wound Dressings and Cosmetic Materials from Bacterial Nanocellulose. In Perspectives in Nanotechnology Series. Bacterial NanoCellulose. CRC Press.

Chawla PR, Bajaj IB, Survase S a., Singhal RS (2009) Microbial cellulose: Fermentative production and applications. Food Technology and Biotechnology, 47, 107-124.

Chen Y, Geng B, Ru J, Tong C, Liu H, Chen J (2017) Comparative characteristics of TEMPO-oxidized cellulose nanofibers and resulting nanopapers from bamboo, softwood, and

hardwood pulps. Cellulose, 24(11), 4831–4844. https://doi.org/10.1007/s10570-017-1478-4

Davidson GF (1948) 6—The acidic properties of cotton cellulose and derived oxycelluloses. Part II. The absorption of methylene blue. Journal of the Textile Institute Transactions, 39(3), T65–T86. https://doi.org/10.1080/19447024808659403

de Santa Maria LC, Santos ALC, Oliveira PC, Barud HS, Messaddeq Y, Ribeiro SJL (2009) Synthesis and characterization of silver nanoparticles impregnated into bacterial cellulose. Materials Letters, 63(9–10), 797–799. https://doi.org/10.1016/j.matlet.2009.01.007

Feng J, Shi Q, Li W, Shu X, Chen A, Xie X, Huang X (2014) Antimicrobial activity of silver nanoparticles in situ growth on TEMPO-mediated oxidized bacterial cellulose. Cellulose, 21(6), 4557–4567. https://doi.org/10.1007/s10570-014-0449-2

Feng QL, Wu J, Chen GQ, Cui FZ, Kim TN, Kim JO (2000) A mechanistic study of the antibacterial effect of silver ions on Escherichia coli and Staphylococcus aureus. Journal of Biomedical Materials Research, 52(4), 662–668. https://doi.org/10.1002/1097-4636(20001215)52:4<662::AID-JBM10>3.0.CO;2-3

Fillat A, Martínez J, Valls C, Cusola O, Roncero MB, Vidal T, Valenzuela S V., Diaz P, Pastor FIJ (2018) Bacterial cellulose for increasing barrier properties of paper products. Cellulose, 25(10), 6093–6105. https://doi.org/10.1007/s10570-018-1967-0

Gao C, Wan Y, Yang C, Dai K, Tang T, Luo H, Wang J (2011) Preparation and characterization of bacterial cellulose sponge with hierarchical pore structure as tissue engineering scaffold. Journal of Porous Materials, 18(2), 139–145. https://doi.org/10.1007/s10934-010-9364-6

Gehmayr V, Potthast A, Sixta H (2012) Reactivity of dissolving pulps modified by TEMPO-mediated oxidation. Cellulose, 19(4), 1125–1134. https://doi.org/10.1007/s10570-012-9729-x

Gert EV, Torgashov VI, Zubets OV, Kaputskii FN (2005) Preparation and Properties of Enterosorbents Based on Carboxylated Microcrystalline Cellulose. Cellulose, 12(5), 517–526. https://doi.org/10.1007/s10570-005-7134-4

Hasan N, Biak DRA, Kamarudin S (2012) Application of Bacterial Cellulose (BC) in Natural Facial Scrub. International Journal on Advanced Science, Engineering and Information Technology, 2(4), 272. https://doi.org/10.18517/ijaseit.2.4.201

551 Ifuku S, Tsuji M, Morimoto M, Saimoto H, Yano H (2009) Synthesis of Silver Nanoparticles
552 Templated by TEMPO-Mediated Oxidized Bacterial Cellulose Nanofibers.
553 Biomacromolecules, 10(9), 2714–2717. https://doi.org/10.1021/bm9006979

554 Inoue Y, Kiyono Y, Asai H, Ochiai Y, Qi J, Olioso A, Shiraiwa T, Horie T, Saito K, Dounagsavanh L
555 (2010) Assessing land-use and carbon stock in slash-and-burn ecosystems in tropical
556 mountain of Laos based on time-series satellite images. International Journal of Applied
557 Earth Observation and Geoinformation, 12(4), 287–297.
558 https://doi.org/10.1016/j.carbpol.2017.02.093

559 Isogai A, Saito T, Fukuzumi H (2011) TEMPO-oxidized cellulose nanofibers. Nanoscale, 3(1),
560 71–85. https://doi.org/10.1039/C0NR00583E

561 Jalili Tabaii M, Emtiazi G (2018) Transparent nontoxic antibacterial wound dressing based on
562 silver nano particle/bacterial cellulose nano composite synthesized in the presence of
563 tripolyphosphate. Journal of Drug Delivery Science and Technology, 44, 244–253.
564 https://doi.org/10.1016/j.jddst.2017.12.019

565 Jaušovec D, Vogrinčič R, Kokol V (2015) Introduction of aldehyde vs. carboxylic groups to
566 cellulose nanofibers using laccase/TEMPO mediated oxidation. Carbohydrate Polymers,
567 116, 74–85. https://doi.org/10.1016/j.carbpol.2014.03.014

568 Jiang J, Ye W, Liu L, Wang Z, Fan Y, Saito T, Isogai A (2017) Cellulose Nanofibers Prepared
569 Using the TEMPO/Laccase/O2 System. Biomacromolecules, 18(1), 288–294.
570 https://doi.org/10.1021/acs.biomac.6b01682

571 Johnson RK, Zink-Sharp A, Glasser WG (2011) Preparation and characterization of
572 hydrophobic derivatives of TEMPO-oxidized nanocelluloses. Cellulose, 18(6), 1599–1609.
573 https://doi.org/10.1007/s10570-011-9579-y

574 Jun YW, Choi JS, Cheon J (2007, March 28) Heterostructured magnetic nanoparticles: Their
575 versatility and high performance capabilities. Chemical Communications, pp. 1203–1214.
576 https://doi.org/10.1039/b614735f

577 Kitaoka T, Isogai A, Onabe F (1999) Chemical modification of pulp fibers by TEMPO-mediated
578 oxidation. Nordic Pulp and Paper Research Journal, 14(04), 279–284.
579 https://doi.org/10.3183/NPPRJ-1999-14-04-p279-284

580 Kong H, Jang J (2008) Antibacterial properties of novel poly(methyl methacrylate) nanofiber
581 containing silver nanoparticles. Langmuir, 24(5), 2051–2056.

https://doi.org/10.1021/la703085e

Lai C, Sheng L, Liao S, Xi T, Zhang Z (2013) Surface characterization of TEMPO-oxidized bacterial cellulose. Surface and Interface Analysis, 45(11–12), 1673–1679. https://doi.org/10.1002/sia.5306

Lansdown ABG (2006) Silver in health care: Antimicrobial effects and safety in use. Current Problems in Dermatology, 33, 17–34. https://doi.org/10.1159/000093928

Lee KY, Buldum G, Mantalaris A, Bismarck A (2014) More than meets the eye in bacterial cellulose: Biosynthesis, bioprocessing, and applications in advanced fiber composites. Macromolecular Bioscience, 14(1), 10–32. https://doi.org/10.1002/mabi.201300298

Liau SY, Read DC, Pugh WJ, Furr JR, Russell AD (1997) Interaction of silver nitrate with readily identifiable groups: Relationship to the antibacterial action of silver ions. Letters in Applied Microbiology, 25(4), 279–283. https://doi.org/10.1046/j.1472-765X.1997.00219.x

Maneerung T, Tokura S, Rujiravanit R (2008) Impregnation of silver nanoparticles into bacterial cellulose for antimicrobial wound dressing. Carbohydrate Polymers, 72(1), 43–51. https://doi.org/10.1016/j.carbpol.2007.07.025

Maria LCS, Santos ALC, Oliveira PC, Valle ASS, Barud HS, Messaddeq Y, Ribeiro SJL (2010) Preparation and antibacterial activity of silver nanoparticles impregnated in bacterial cellulose. Polímeros, 20(1), 72–77. https://doi.org/10.1590/S0104-14282010005000001

Marini M, De Niederhausern S, Iseppi R, Bondi M, Sabia C, Toselli M, Pilati F (2007) Antibacterial Activity of Plastics Coated with Silver-Doped Organic−Inorganic Hybrid Coatings Prepared by Sol−Gel Processes. Biomacromolecules, 8(4), 1246–1254. https://doi.org/10.1021/bm060721b

Matsumoto A, Ishikawa T, Odani T, Oikawa H, Okada S, Nakanishi H (2006) An organic/inorganic nanocomposite consisting of polymuconate and silver nanoparticles. Macromolecular Chemistry and Physics, 207(4), 361–369. https://doi.org/10.1002/macp.200500430

Miao C, Hamad WY (2013) Cellulose reinforced polymer composites and nanocomposites: a critical review. Cellulose, 20(5), 2221–2262. https://doi.org/10.1007/s10570-013-0007-3

Milanović J, Mihajlovski K, Nikolić T, Kostić M (2016) Antimicrobial Cotton Fibers Prepared By Tempo-Mediated Oxidation and Subsequent Silver Deposition. Cellulose Chem. Technol,

613 50(910), 905–914.

614 Nimeskern L, Martínez Ávila H, Sundberg J, Gatenholm P, Müller R, Stok KS (2013) Mechanical
615 evaluation of bacterial nanocellulose as an implant material for ear cartilage
616 replacement. Journal of the Mechanical Behavior of Biomedical Materials, 22, 12–21.
617 https://doi.org/10.1016/j.jmbbm.2013.03.005

618 Pahlevan M, Toivakka M, Alam P (2018) Mechanical properties of TEMPO-oxidised bacterial
619 cellulose-amino acid biomaterials. European Polymer Journal, 101, 29–36.
620 https://doi.org/10.1016/j.eurpolymj.2018.02.013

621 Patel I, Ludwig R, Haltrich D, Rosenau T, Potthast A (2011) Studies of the chemoenzymatic
622 modification of cellulosic pulps by the laccase-TEMPO system. Holzforschung, 65(4),
623 475–481. https://doi.org/10.1515/HF.2011.035

624 Perala SRK, Kumar S (2013) On the mechanism of metal nanoparticle synthesis in the Brust-
625 Schiffrin method. Langmuir, 29(31), 9863–9873. https://doi.org/10.1021/la401604q

626 Pinto RJB, Marques PAAP, Neto CP, Trindade T, Daina S, Sadocco P (2009) Antibacterial
627 activity of nanocomposites of silver and bacterial or vegetable cellulosic fibers. Acta
628 Biomaterialia, 5(6), 2279–2289. https://doi.org/10.1016/j.actbio.2009.02.003

629 Quintana E, Roncero MB, Vidal T, Valls C (2017) Cellulose oxidation by Laccase-TEMPO
630 treatments. Carbohydrate Polymers, 157, 1488–1495.
631 https://doi.org/10.1016/j.carbpol.2016.11.033

632 Rol F, Belgacem MN, Gandini A, Bras J (2019, January) Recent advances in surface-modified
633 cellulose nanofibrils. Progress in Polymer Science, Vol. 88, pp. 241–264.
634 https://doi.org/10.1016/j.progpolymsci.2018.09.002

635 Saito T, Shibata I, Isogai A, Suguri N, Sumikawa N (2005) Distribution of carboxylate groups
636 introduced into cotton linters by the TEMPO-mediated oxidation. Carbohydrate
637 Polymers, 61(4), 414–419. https://doi.org/10.1016/j.carbpol.2005.05.014

638 Saito Tsuguyuki, Isogai A (2004) TEMPO-mediated oxidation of native cellulose. The effect of
639 oxidation conditions on chemical and crystal structures of the water-insoluble fractions.
640 Biomacromolecules, 5(5), 1983–1989. https://doi.org/10.1021/bm0497769

641 Saito T, Isogai A (2005) A novel method to improve wet strength of paper. Tappi Journal, 4(3),
642 3–8.

643 Saito T, Isogai A (2006) Introduction of aldehyde groups on surfaces of native cellulose fibers
644 by TEMPO-mediated oxidation. Colloids and Surfaces A: Physicochemical and
645 Engineering Aspects, 289(1–3), 219–225. https://doi.org/10.1016/j.colsurfa.2006.04.038

646 Scott WE (1996) Wet strength additives. In Principles of wet end chemistry (pp. 61–68).
647 Retrieved from http://www.tappi.org/content/pdf/member_groups/paper/0101r241.pdf

648 Shao W, Liu H, Liu X, Sun H, Wang S, Zhang R (2015) pH-responsive release behavior and anti-
649 bacterial activity of bacterial cellulose-silver nanocomposites. International Journal of
650 Biological Macromolecules, 76, 209–217. https://doi.org/10.1016/j.ijbiomac.2015.02.048

651 Sondi I, Salopek-Sondi B (2004) Silver nanoparticles as antimicrobial agent: A case study on E.
652 coli as a model for Gram-negative bacteria. Journal of Colloid and Interface Science,
653 275(1), 177–182. https://doi.org/10.1016/j.jcis.2004.02.012

654 Spence KL, Venditti RA, Habibi Y, Rojas OJ, Pawlak JJ (2010) The effect of chemical
655 composition on microfibrillar cellulose films from wood pulps: mechanical processing and
656 physical properties. Bioresource Technology, 101(15), 5961–5968.
657 https://doi.org/10.1016/j.biortech.2010.02.104

658 Stumpf TR, Yang X, Zhang J, Cao X (2018, January 1) In situ and ex situ modifications of
659 bacterial cellulose for applications in tissue engineering. Materials Science and
660 Engineering C, Vol. 82, pp. 372–383. https://doi.org/10.1016/j.msec.2016.11.121

661 Tolvaj L, Faix O (1995) Artificial Ageing of Wood Monitored by DRIFT Spectroscopy and CIE
662 L*a*b* Color Measurements 1. Effect of UV Light. Holzforschung, 49(5), 397–404.
663 https://doi.org/10.1515/hfsg.1995.49.5.397

664 Uddin KMA, Lokanathan AR, Liljeström A, Chen X, Rojas OJ, Laine J (2014) Silver nanoparticle
665 synthesis mediated by carboxylated cellulose nanocrystals. Green Materials, 2(4), 183–
666 192. https://doi.org/10.1680/gmat.14.00010

667 Ul-Islam M, Khan S, Ullah MW, Park JK (2015) Bacterial cellulose composites: Synthetic
668 strategies and multiple applications in bio-medical and electro-conductive fields.
669 Biotechnology Journal, 10(12), 1847–1861. https://doi.org/10.1002/biot.201500106

670 Ullah H, Santos HA, Khan T (2016) Applications of bacterial cellulose in food, cosmetics and
671 drug delivery. Cellulose, 23(4), 2291–2314. https://doi.org/10.1007/s10570-016-0986-y

672 Ullah H, Wahid F, Santos HA, Khan T (2016) Advances in biomedical and pharmaceutical
673 applications of functional bacterial cellulose-based nanocomposites. Carbohydrate

674 Polymers, 150, 330–352. https://doi.org/10.1016/j.carbpol.2016.05.029

675 Wu C-N, Fuh S-C, Lin S-P, Lin Y-Y, Chen H-Y, Liu J-M, Cheng K-C (2018) TEMPO-Oxidized
676 Bacterial Cellulose Pellicle with Silver Nanoparticles for Wound Dressing.
677 Biomacromolecules, 19(2), 544–554. https://doi.org/10.1021/acs.biomac.7b01660

678 Wu Q, Cao H, Luan Q, Zhang J, Wang Z, Warner JH, Watt AAR (2008) Biomolecule-assisted
679 synthesis of water-soluble silver nanoparticles and their biomedical applications.
680 Inorganic Chemistry, 47(13), 5882–5888. https://doi.org/10.1021/ic8002228

681 Wu Y, Wang F, Huang Y (2018) Facile and simple fabrication of strong, transparent and
682 flexible aramid nanofibers/bacterial cellulose nanocomposite membranes. Composites
683 Science and Technology, 159, 70–76. https://doi.org/10.1016/j.compscitech.2018.02.036

684 Yang G, Xie J, Deng Y, Bian Y, Hong F (2012) Hydrothermal synthesis of bacterial
685 cellulose/AgNPs composite: A “green” route for antibacterial application. Carbohydrate
686 Polymers, 87(4), 2482–2487. https://doi.org/10.1016/j.carbpol.2011.11.017

687 Yano H, Sugiyama J, Nakagaito AN, Nogi M, Matsuura T, Hikita M, Handa K (2005) Optically
688 Transparent Composites Reinforced with Networks of Bacterial Nanofibers. Advanced
689 Materials, 17(2), 153–155. https://doi.org/10.1002/adma.200400597

690 Zhou Q, Zhang Q, Wang P, Deng C, Wang Q, Fan X (2017) Enhancement biocompatibility of
691 bacterial cellulose membrane *via* laccase/TEMPO mediated grafting of silk fibroins.
692 Fibers and Polymers, 18(8), 1478–1485. https://doi.org/10.1007/s12221-017-7306-5

693 Zhou Y, Yu SH, Thomas A, Han BH (2003) In situ cyclodextrin-based homogeneous
694 incorporation of metal (M = Pd, Pt, Ru) nanoparticles into silica with bimodal pore
695 structure. Chemical Communications, 9(2), 262–263. https://doi.org/10.1039/b210590j

696

697